Multi-Objective Optimization of Daylight in Building Skin Guided by Lingnan Traditional Wisdom

Haixiu Liang[1,2,*] and Dongyuan Guo[1]

[1] South China University of Technology, School of Architecture, Guangzhou, 510641, China
[2] Architectural Design & Research Institute of SCUT Co., Ltd., Guangzhou, 510641, China

*lianghaixiu@scut.edu.cn

Abstract. While multi-objective optimization (MOO) gains traction in building performance, traditional strategies—like historic daylight-ventilation-shading designs—are sidelined as mere decorations, with untapped environmental potential and limited computational integration.

This study bridges this gap via a Lingnan heritage-MOO envelope framework targeting UDI, GA, and illuminance CV. Parametric modeling converts traditional geometric features into computable rules for designer-guided optimization. Key variables (gradient patterns, porosity, spatial configurations) are simulated in Grasshopper with NSGA-II, generating Pareto solutions analyzed by k-means clustering.

Case results show optimized envelopes improve UDI, GA, and uniformity while retaining traditional aesthetics. The research presents a "heritage-performance" integration approach, offering early-stage methods to merge high-performance design with architectural tradition.

Keywords: Multi-Objective Optimization; Daylight; Parametric Design

1 Introduction

Against the backdrop of global energy shortages and escalating climate change challenges, in the construction industry—a major energy-consuming sector—architects are increasingly enhancing effective daylighting to improve comfort while reducing energy consumption. This strategy has proven effective across various building types [1]. However, designing spaces with optimal daylighting presents significant challenges, involving a trade-off between the comfort provided by daylight and energy efficiency. Evaluation and prediction of daylight performance is essential, especially in the early design stages [2].

While performance simulation excels in quantitative analysis, recent research increasingly integrates traditional architectural wisdom to modernize regional energy-efficient concepts. For example, Zhiwei Zeng et al. [3] used CFD simulations to validate summer wind optimization in Kaiping Mashilong Village's "comb-layout + front-pond-rear-village" pattern. Hiroyuki Shinohara et al. [4] developed computational designs

K. Chulsoo et al. (eds.), *Proceedings of the 2025 4th International Conference on Art Design and Digital Technology (ADDT 2025)*, Advances in Computer Science Research 123,
https://doi.org/10.2991/978-94-6463-815-8_38

inspired by Kagome bamboo weaving, exploring its self-supporting and geometric potentials at architectural scales to merge tradition with modern design.

However, complex architectural design practices face challenges in multi-objective coordination, as single-dimensional optimization struggles to maximize overall benefits. Recently, multi-objective optimization methods have been widely applied. Liu et al. [5] considered energy use and occupant comfort as optimization objectives for typical building cases in China. Liang [6] used lighting, cooling, and heating energy demands as optimization targets for high-rise design.

This study parametrizes traditional geometric logic into computable variables via modeling, integrates them with daylight metrics to develop a multi-objective optimization framework, and provides a new quantitative approach to balance performance optimization and traditional culture in architectural design.

2 Method

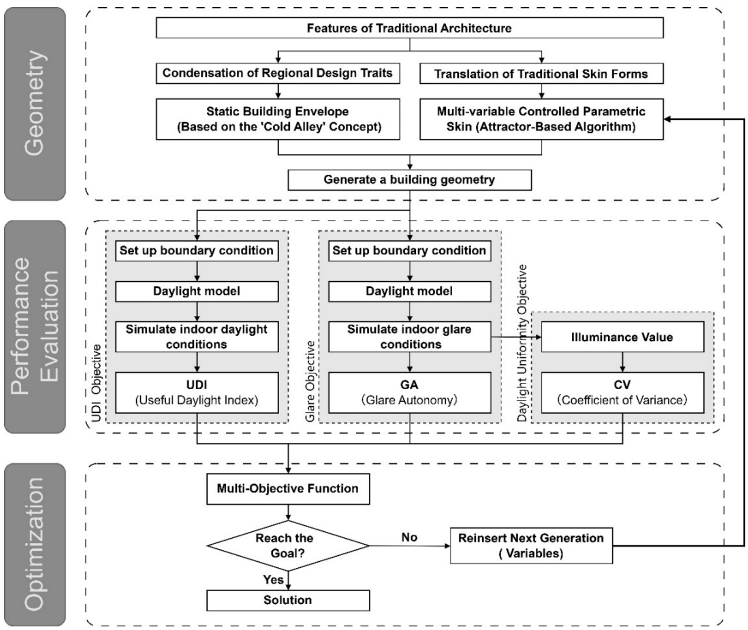

Fig. 1. Overall Process

The overall process is summarized in Fig.1, aiming to optimize the atrium skin system to achieve maximized indoor daylighting, daylight uniformity, and minimized glare. The methodology of this paper is divided into three parts: parametric model development, performance evaluation, and multi-objective optimization.

The first step involves preparing a parametric skin system model integrating traditional craftsmanship (taking "Lingnan oyster shell windows" as an example) and a skin porosity gradient control system using a hierarchical agent system. In traditional multi-objective optimization, conventional "variable-performance" simulations often lead to skin forms fully determined by algorithms, lacking form controllability. Thus, this study uses an attractor-based algorithm for parametric skin generation: intersecting lines of multi-degree-of-freedom planes and geometric forms act as attractors to influence porosity, creating rhythmical parametric skins while providing diverse data for multi-objective optimization.

Once the geometry is defined, the next step is to simulate the model to obtain performance data. Using performance simulation tools such as Ladybug and Honeybee on the Grasshopper platform[7], simulations and calculations are conducted for Useful Daylight Illuminance (UDI 100-2000), Glare Autonomy (GA), and daylight uniformity (Coefficient of Variation, CV).

3 Case Study

3.1 Parametric Façade Development

This study parametrically models Lingnan oyster-shell windows, integrating wind-simulated atrium geometry for a performance-culture skin. Grasshopper's attractor-porosity algorithm uses rotatable control planes (P1/P2) to define form axes, with positions/angles controlling symmetrical rhythms. A distance-based system assigns porosity inversely to attractor proximity—closer areas denser, farther sparser—via grid parameters. This translates cultural motifs into density rules, creating epidermal morphologies where porosity gradients highlight attractor focal axes (e.g., central symmetry) for 12-variable optimization (Table 1).

Table 1. Overview of Variable Parameters

Façade	U	V	X-Y-Z Euler angles (P1)	Z1(P1)	X-Y-Z Euler angles (P2)	Z2(P2)	Minimum Porosity (%)	Maximum Porosity (%)
Case1	10	10	-26.26;35.64; -71.77	9.4	27.46; -85.91; -45.70	5.7	0.2	0.54

3.2 Daylight Performance Evaluation

This study uses Useful Daylight Illuminance (UDI) to evaluate daylighting potential. UDI refers to the percentage of occupied time during which test points achieve specific lux levels within three illuminance ranges.

$$UDI = \frac{\sum_i (wf_i t_i)}{\sum_i t_i} \epsilon[0,1] \; with \; wf_i =$$

$$\begin{cases} UDI_{Over\ limit} \ With\ wf_i = \begin{cases} 1 \ if \ E_{Daylight} > E_{Upper\ limit} \\ 0 \ if \ E_{Daylight} \le E_{Upper\ limit} \end{cases} \\ UDI_{Useful} \ With\ wf_i = \begin{cases} 1 \ if \ E_{Lower\ limit} \le E_{Daylight} < E_{Upper\ limit} \\ 0 \ if \ E_{Daylight} < E_{Lower\ limit} \vee E_{Daylight} > E_{Upper\ limit} \end{cases} \\ UDI_{Under\ limit} \ With\ wf_i = \begin{cases} 1 \ if \ E_{Daylight} < E_{Upper\ limit} \\ 1 \ if \ E_{Daylight} \ge E_{Upper\ limit} \end{cases} \end{cases} \tag{1}$$

Glare (G) is a complex visual discomfort phenomenon used to evaluate or predict potential discomfort events. Wienold et al. improved the glare calculation formula by proposing the Daylight Glare Probability.

$$DGP = 5.87 * 10^5 E_v + 0.0918 * \log_{10}\left[\sum_{i=1}^{n}\left(\frac{L_{si}^2 * \omega_{si}}{E_v^{1.87} * P_i^2}\right)\right] + 0.16 \quad (2)$$

Jones introduced a climate-based image-free annual glare simulation method (image-free DGP, iDGP). Based on the iDGP method, Jones proposed indices of Glare Autonomy (GA). According to the UGP scale in EN17037:2018, the threshold is set at 0.4 [8].

$$GA = \frac{\sum_i (wf_i t_i)}{\sum_i (t_i)} \epsilon[0,1] \; with \; wf_i = \begin{cases} 1 \; if \; DGP \le DGP_{limit} \\ 1 \; if \; DGP > DGP_{limit} \end{cases} \quad (3)$$

Armstrong introduced the Coefficient of Variation (CV) as a standard for assessing illuminance uniformity [9]. This metric evaluates uniformity by considering illuminance values at all points through statistical methods, mitigating outlier influence, with CV used to analyze work plane daylighting uniformity.

$$CV = \frac{S}{E_{avg}} \; with \; S = \sqrt{\frac{\sum\left(E_i - E_{avg}\right)^2}{n}} \quad (4)$$

3.3 Multi-Objective Optimization (MOO)

This study employs the Non-dominated Sorting Genetic Algorithm II (NSGA-II)—an evolutionary algorithm optimizing candidate solutions against Pareto front constraints via subpopulation similarity evaluation to generate diverse non-dominated solutions for multi-objective optimizations [10]. The objective functions are as follows:

$$\min_{x \epsilon X} f(x) = [f_1(x), f_2(x), f_3(x)] \quad (5)$$

The test aims to minimize three objectives: $f_1(x)$, the reciprocal of the mean UDI across measurement points (to facilitate minimization in the MMO framework); $f_2(x)$, the coefficient of variation (CV) of daylighting, quantifying uniformity differences; and$f_3(x)$, the reciprocal of the mean GA across measurement points.

$$f_1(x) = \frac{1}{\left(\frac{\sum_{i=1}^{n}(UDI_{100-2000})n}{n}\right) \div 100} \quad (6)$$

$$f_2(x) = CV \quad (7)$$

$$f_3(x) = \frac{1}{\left(\frac{\sum_{i=1}^{n}(GA)n}{n}\right) \div 100} \quad (8)$$

4 Test Results

4.1 Judgment of Result Convergence

With preliminary optimization parameter settings, 22 optimization schemes were generated per generation. The NSGA-II optimization algorithm performed stochastic crossover operations on the results to generate the next generation of schemes. After 30 generations of iteration and 15 hours of computation, a total of 660 schemes were generated (Fig.2).

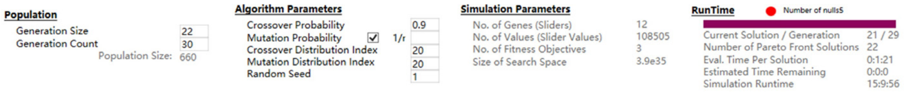

Fig. 2. Multi-Objective Optimization Settings

Data analysis of the 660 optimized schemes reveals: In the parallel coordinate plot (Fig. 3(a)), darker blue curves correspond to schemes closer to the final optimization generation, with their Y-axis coordinates approaching optimal values. Fig. 3(b) presents the value repetition analysis: on the Y-axis, longer horizontal lines indicate higher repetition frequencies of the corresponding values.

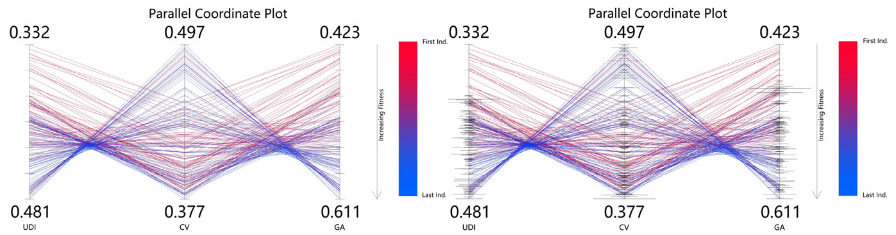

a b

Fig. 3. (a) Parallel Coordinate Plot (b) Repeated Optimization Values Plot

Fig. 4 presents the Fitness Graph for optimization objectives: smaller Y-axis value dispersion indicates superior optimization outcomes. Fig. 5's Standard Deviation Plot tracks iterative objective solutions: the leftward shift of the red-to-blue curve signifies generational mean reduction. The convergent trend of results validates experimental reliability, rendering the data suitable for subsequent research.

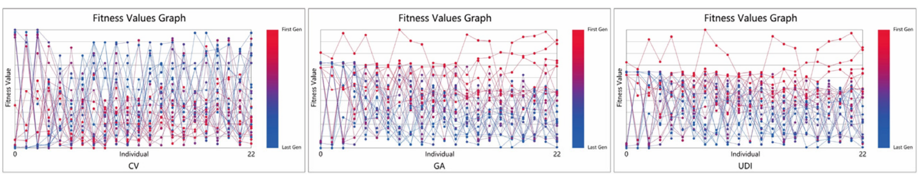

Fig. 4. Fitness Values Graph

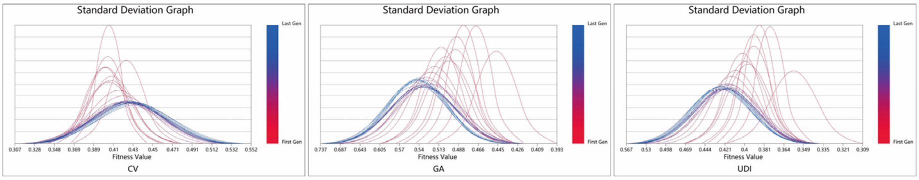

Fig. 5. Standard Deviation Graph

4.2 Pareto Solution Set Analysis

Pareto optimal solutions for daylight performance multi-objective optimization balance UDI, GA, and CV, but objective conflicts lead to varying indicator weightings across solutions. Using K-means, this study clusters all Pareto solutions into three groups (Fig. 6): C1 (15 solutions), C2 (18 solutions), and C3 (17 solutions).

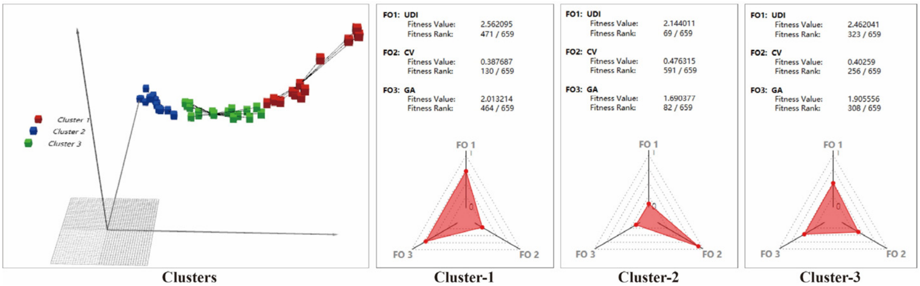

Fig. 6. Clustering of Pareto Solutions

The first cluster (G5-20) prioritizes high annual daylight uniformity but lower UDI/GA; the second (G29-12) features high UDI/GA but poor uniformity; the third (G29-19) shows balanced performance with all metrics above average, as indicated in the cluster plot.

For Cluster 3—a Pareto solution set with balanced overall optimization in the above clustering analysis—the 17 envelope forms were generated via the Wallacei platform. G29-19 was ultimately selected as the target envelope, which integrates modern technology with traditional patterns while optimizing daylight performance and practicing the concept of sustainable development (see Fig. 7).

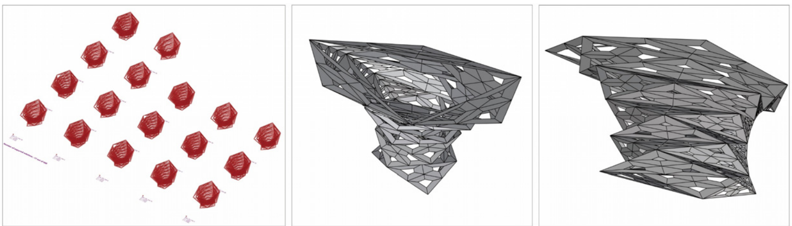

Fig. 7. Pareto solution set of Cluster 3 and the selected G29-19

5 Conclusion

This study presents a framework integrating Lingnan traditional architectural wisdom with multi-objective optimization (MOO), translating "cold alley" designs into a Grasshopper parametric workflow with a 12-variable system. A South China case using NSGA-II shows optimized envelopes retain traditional symmetrical/gradient aesthetics while improving efficiency and illuminance uniformity. However, potential challenges remain for practical implementation, including construction complexity, cost implications, and stylistic coordination with diverse traditional contexts—areas warranting further exploration in future research. The research validates MOO's potential for merging heritage and performance, suggesting future expansions to thermal comfort, material cost optimization, and machine learning-aided workflows as critical frontiers for sustainable regional architecture.

References

1. Bakmohammadi, P., Noorzai, E.: Optimization of the design of the primary school classrooms in terms of energy and daylight performance considering occupants' thermal and visual comfort. Energy Rep. 6 (2020), 1590–1607.
2. De Wilde, P.: Building Performance Analysis. John Wiley & Sons (2018).
3. Zeng, Z., Li, L., Pang, Y.: Analysis on climate adaptability of traditional villages in Lingnan, China—World Cultural Heritage Site of Majianglong Villages as example. In: *Procedia Engineering*, pp. 2011–2018. (2017).
4. Shinohara, H., Chan, T.H.P.: A computation design method for architectural artifacts adapted from traditional Kagome bamboo basketry techniques. Frontiers of Architectural Research 13(2) (2024), 249–264.
5. Liu, C.Q., Wang, B., Ma, Y., Wu, Z.B.: Multi-objective optimization design of high-rise diagrid structure based on Non-dominated Sorting Genetic Algorithm II. J. Build. Eng. 112801 (2025).
6. Liang, M., Xu, M., Wang, S.: A novel multi-objective evolutionary algorithm for transit network design and frequency-setting problem considering passengers' choice behaviors under station congestion. Transportation Research Part B: Methodological 197 (2025), 103238.
7. Grasshopper. https://www.grasshopper3d.com/ (2020). (Accessed 31 May 2020).
8. Wang, Y., Sun, Y., Lu, P., Berta, M.: An integrated climate-based daylight performance evaluation framework for indoor arenas' roof system. J. Build. Eng. 90 (2024), 109164.
9. Brownlee, J.: Clever Algorithms. https://github.com/clever-algorithms/CleverAgorithms (2012). (Accessed 31 May 2020).
10. Robert McNeel & Associates: Rhinoceros. https://www.rhino3d.com/ (2020). (Accessed 31 May 2020).